Effects of interaction strength, doping, and frustration on the antiferromagnetic phase of the two-dimensional Hubbard model

L. Fratino,[1] M. Charlebois,[2] P. Sémon,[3] G. Sordi,[1,*] and A.-M. S. Tremblay[2,4]

[1]*Department of Physics, Royal Holloway, University of London, Egham, Surrey TW20 0EX, United Kingdom*

[2]*Département de Physique, Institut Quantique, and Regroupement Québécois sur les Matériaux de Pointe, Université de Sherbrooke, Sherbrooke, Québec, Canada J1K 2R1*

[3]*Computational Science Initiative, Brookhaven National Laboratory, Upton, New York 11973-5000, USA*

[4]*Canadian Institute for Advanced Research, Toronto, Ontario, Canada M5G 1Z8*

Recent quantum-gas microscopy of ultracold atoms and scanning tunneling microscopy of the cuprates reveal new detailed information about doped Mott antiferromagnets, which can be compared with calculations. Using cellular dynamical mean-field theory, we map out the antiferromagnetic (AF) phase of the two-dimensional Hubbard model as a function of interaction strength U, hole doping δ, and temperature T. The Néel phase boundary is nonmonotonic as a function of U and δ. Frustration induced by second-neighbor hopping reduces Néel order more effectively at small U. The doped AF is stabilized at large U by kinetic energy and at small U by potential energy. The transition between the AF insulator and the doped metallic AF is continuous. At large U, we find in-gap states similar to those observed in scanning tunneling microscopy. We predict that, contrary to the Hubbard bands, these states are only slightly spin polarized.

The quantum mechanics of interacting electrons on a lattice can lead to complex many-body phase diagrams. For example, doping a layered Mott insulator can give rise to antiferromagnetism, pseudogap, unconventional superconductivity, and multiple exotic phases [1]. The Hubbard model is the simplest model of interacting electrons on a lattice. It can be used for both natural (e.g., cuprates) and artificial (e.g., ultracold atoms) systems [2–5]. Therefore, understanding the phases that appear in this model and the transitions between them is a central program in condensed matter physics.

Here, we study the regimes where antiferromagnetic (AF) correlations set in within the two-dimensional (2D) Hubbard model on a square lattice as a function of interaction U, doping δ, and temperature T, within cellular dynamical mean-field theory (CDMFT) [6–8]. The motivation for our work is threefold. First, recent advances in ultracold-atom experiments can now reach temperatures low enough to detect AF correlations for repulsively interacting Fermi gases [9–15]. Hence, a theoretical characterization of the AF phase in the whole U-δ-T space might guide ultracold-atom experiments that are exploring this uncharted territory. Second, recent tunneling spectroscopy studies [16,17] reveal new details on the evolution of the AF Mott insulator upon doping, thus calling for theoretical explanations. Third, on the theory side, we still know little about the detailed boundaries of the AF phase in the whole U-δ-T space of the 2D Hubbard model and the mechanism by which AF is stabilized. Most previous studies with this and other methods focused on $T = 0$ [18–23]. At finite doping, or with frustration, methods based on quantum Monte Carlo generally have a sign problem [6,24–30]. Our results might serve as a stepping stone for different approaches directed towards including Mott physics and long-wavelength fluctuations [31–34].

Model and method. We consider the 2D Hubbard model, $H = -\sum_{ij\sigma} t_{ij} c_{i\sigma}^{\dagger} c_{j\sigma} + U \sum_i n_{i\uparrow} n_{i\downarrow} - \mu \sum_{i\sigma} n_{i\sigma}$, where $t_{ij} = t(t')$ is the (next-) nearest-neighbor hopping, U is the on-site Coulomb repulsion, and μ is the chemical potential. Here, $c_{i\sigma}^{\dagger}$ ($c_{i\sigma}$) is the creation (destruction) operator on lattice site i and spin σ, and $n_{i\sigma}$ is the number operator. We set $t = 1$ as our energy unit. Within the cellular extension [6–8] of dynamical mean-field theory [36], a 2×2 plaquette is embedded in a self-consistent bath. We have successfully benchmarked this approach [37] at $\delta = 0$, where reliable results are available.

We solve the cluster impurity problem using continuous time quantum Monte Carlo based on the expansion of the hybridization between impurity and bath [38,39]. Symmetry breaking is allowed only in the bath. It is efficient to use of the C_{2v} group symmetry with mirrors along plaquette diagonals [37,40,41].

U-T-δ map of the AF phase. Long-wavelength spin fluctuations lead, in two dimensions, to a vanishing staggered magnetization m_z at finite temperature [42,43]. Nevertheless, $m_z = \frac{2}{N_c} \sum_i (-1)^i (n_{i\uparrow} - n_{i\downarrow})$ is nonzero in cold-atom experiments because of finite-size effects. For cuprates, the m_z that we compute becomes nonvanishing at a dynamical mean-field Néel temperature T_N^d where the antiferromagnetic correlation length of the infinite system would start to grow exponentially [37]. Coupling in the third dimension leads to true long-range order at a lower temperature.

As a first step, m_z is used to map out the AF phase in the U-T-δ space for $t' = -0.1$. We consider hole doping only ($\delta = 1 - n > 0$) and perform various cuts, i.e., (i) at $\delta = 0$ [T-U plane in Fig. 1(b)], (ii) at fixed values of U [T-δ planes in Figs. 1(c) and 1(d)], and (iii) at fixed temperature T [δ-U plane at $T = 1/10$ in Fig. 1(e)]. These cuts are reported in the U-T-δ space in Fig. 1(a), where one sees that $T_N^d(U,\delta)$ has a global maximum at $U \approx 7$ for $\delta = 0$. The sign problem prevents convergence below $T \approx 1/20$. The value of $m_z \neq 0$ is

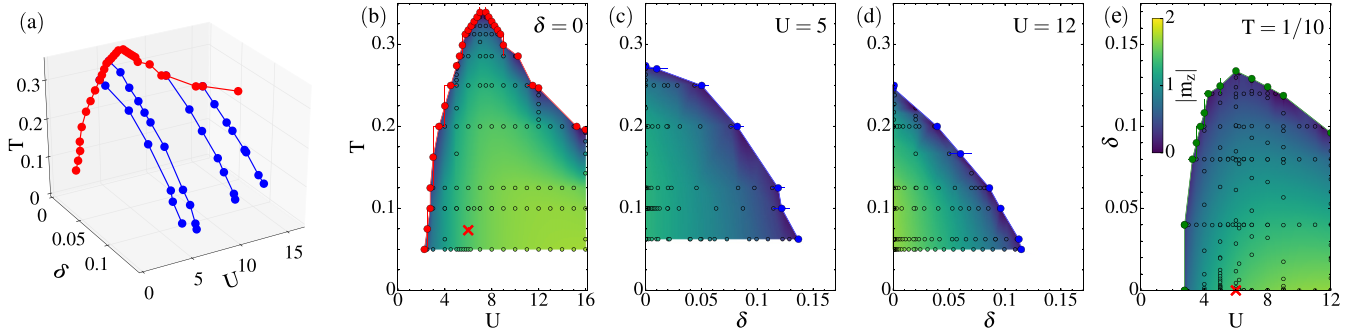*Corresponding author: giovanni.sordi@rhul.ac.uk

FIG. 1. (a) AF phase of the 2D Hubbard model in the U-T-δ space, for $t' = -0.1$. (b) T-U cut at $\delta = 0$. (c) T-δ cut for $U = 5$ and (d) $U = 12$. (e) δ-U cut for $T = 1/10$. The magnitude of m_z is color coded [see SM [35] for $m_z(U)$ and $m_z(\delta)$ curves at different temperatures]. The paramagnetic to AF phase boundary is drawn where $m_z < 0.045$. The red cross in (b) and (e) indicates the position of the Mott critical endpoint $(U_{\mathrm{MIT}}, T_{\mathrm{MIT}})$ in the underlying normal phase.

color coded in Figs. 1(b)–1(e) and shown in the Supplemental Material (SM) [35].

The staggered magnetization $m_z(U, \delta, T)$ is largest in the $\delta = 0$ plane and saturates for large U and low T, as in mean field [44]. Our analysis of the AF region in the U-T-δ space highlights two points. First, the overall behavior of m_z differs from that of T_N^d: For example, $m_z(U, T = 0)|_{\delta=0}$ does not scale with either $T_N^d(U)|_{\delta=0}$ [phase boundary in Fig. 1(b)], or with $\delta_N^d(U)|_T$ [phase boundary in Fig. 1(e)]. Physically, even if large U creates local moments, T_N^d decreases with U since it is the superexchange $J = 4t^2/U$ that aligns these moments at finite temperature. Second, the maxima [45,46] of both $T_N^d(U)|_{\delta=0}$ and $\delta_N^d(U)|_T$ are correlated with the Mott transition that exists at $\delta = 0$ in the unstable normal state below T_N^d, suggesting that the hidden Mott transition [see the Mott endpoint in Figs. 1(b) and 1(e)] drives the qualitative changes in the AF state.

It is well known that the increase of $T_N^d(U)$ at small U is explained by the Slater physics of nesting and that the decrease of $T_N^d(U)$ at large U is explained by the Heisenberg physics of superexchange. Hence, the fact that the position of the maximum of $T_N^d(U)$ at $\delta = 0$ is controlled by the underlying Mott transition [37] reflects the underlying physics. As we saw above [cf. green line in Fig. 1(e)], this difference between small and large U persists upon doping since the range of δ where AF exists first increases with U and then decreases, with the crossover again controlled by the Mott transition at $\delta = 0$. In contrast, regardless of the strength of U, $T_N^d(\delta)$ monotonically decreases with increasing δ [phase boundaries in Figs. 1(c) and 1(d)].

Effect of frustration on $T_N^d(U, \delta)$. We can gain further insights by varying the next-nearest-neighbor hopping t', which frustrates AF order in varying degrees depending on the value of U, as we shall see. Having in mind the physics of hole-doped cuprates, here we consider only negative values of t', in the range $t' \in [0, -0.5]$.

Figure 2(a) shows $T_N^d(U)$ at $\delta = 0$ for different values of t'. AF now appears at a critical U_c that shifts to higher values of U upon increasing $|t'|$, in agreement with expectation from the physics of nesting and also from the $T = 0$, DMFT $d = \infty$ [48,49], and Hartree-Fock (HF) results [47]. The $T \to 0$ transition at U_c is consistent with first order [47–49] for finite t' (see Fig. 2 in SM [35]). U_c is larger than the HF result [47] because the vertex is renormalized downward

compared to the bare U by fluctuations in other channels [50–53]. We find once again that the position of max $T_N^d(U)$ is correlated with the Mott transition in the underlying normal state.

Although frustration reduces $T_N^d(U)$ as expected, the reduction of $T_N^d(U)$ upon increasing $|t'|$ at $\delta = 0$ is stronger at small U than at large U, as shown in Fig. 2(b). Indeed, although at small U deviations from perfect nesting are first order in $|t'/t|$, at large U the AF arises from localized spins and the correct quantities to compare are $J' = 4t'^2/U$ and $J = 4t^2/U$ whose ratio scales as $|t'/t|^2$. Figure 2(c) shows the doping-dependent $T_N^d(\delta)$ at $U = 16$ for different values of t': At our lowest temperature, a fivefold increase of $|t'|$ only approximately halves the critical doping δ_N^d at which the AF phase ends. When T_N^d is large at half filling, the AF phase extends farther in doping. The transition at the critical δ is consistent with second order (see Fig. 1(d) in SM [35]).

AF insulator to AF metal transition. Having mapped out the Néel state, we next explore its nature by analyzing the local density of states (DOS) $N(\omega)$ and the occupation $n(\mu) = 1 - \delta(\mu)$.

First, consider the $\delta = 0$ case. For $t' = 0$ we know that CDMFT recovers the AF insulating behavior [37]. In principle, at small U and large t', the AF state can have both hole pockets and electron pockets at the Fermi surface. Then the AF state would be metallic even at $\delta = 0$ [47,53]. Here, we find that the $\delta = 0$ solution is insulating for all t' and U we considered. This can be checked from the local DOS and from the occupation shown at $t' = -0.1$ for $U = 5$ and $U = 12$ in Fig. 3. More specifically, the plateau in the occupation at $n(\mu) = 1$ in Figs. 3(c) and 3(g) signals an incompressible insulator, i.e., the charge compressibility $\kappa = n^{-2} dn/d\mu$ vanishes.

Second, consider the AF state at finite doping $\delta \neq 0$. In this case, $n(\mu)$ has a finite slope, signaling a compressible metal, i.e., $\kappa > 0$. In addition, Figs. 3(a) and 3(e) show that the local DOS has a small but finite spectral weight at the Fermi level, indicating a metallic state.

Therefore, at $\delta = 0$ there is an AF insulator (AF-I), whereas at $\delta > 0$ there is an AF metal (AF-M). This also holds in the $d \to \infty$ limit [54]. What is the nature of the AF-I to AF-M transition driven by doping? Close to $n(\mu) = 1$ ($\delta = 1 - n = 0$), the occupation $n(\mu)$ is continuous for all T we have explored. As T decreases, the curvature at the
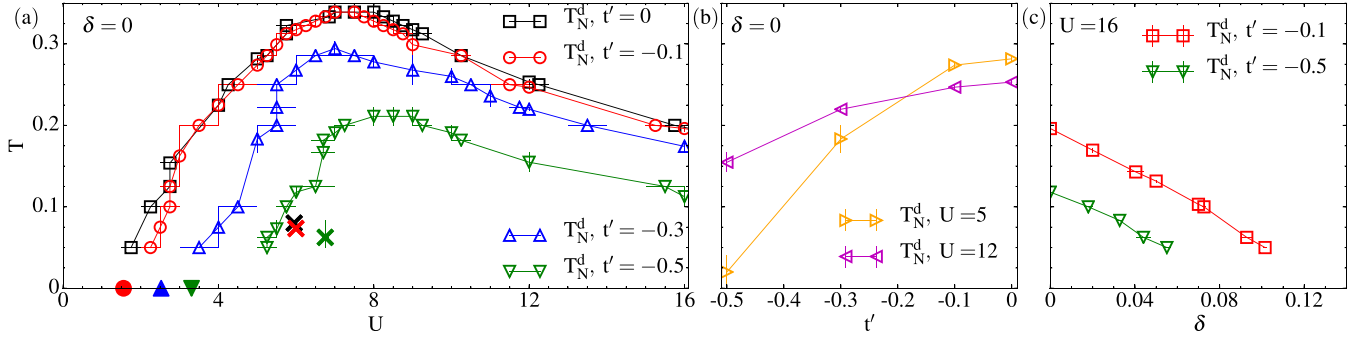
FIG. 2. (a) T_N^d for $t' = 0, -0.1, -0.3, -0.5$. As a reference, we show with solid symbols the $T = 0$ Hartree-Fock results of Ref. [47] for the critical U of the AF onset. Crosses indicate the Mott endpoints in the underlying normal phase: Data are for $t' = 0$ (black), $t' = -0.1$ (red), and $t' = -0.5$ (green). (b) T_N^d vs t' at $\delta = 0$ for $U = 5, 12$. (c) T_N^d vs δ at $U = 16$ for $t' = -0.1, -0.5$.

transition becomes sharper, suggesting a discontinuous change in slope in the $T = 0$ limit, as expected for a second-order AF-I to AF-M transition. The transition is a crossover at finite T.

Density of states and "in-gap" states. There are striking differences between the DOS $N(\omega)$ of a doped Slater AF ($U = 5$) versus a doped Mott AF ($U = 12$).

For $U = 5$, the $N(\omega)$ spectra for $\delta = 0$ in Fig. 3(a) shows two Bogoliubov peaks along with high-frequency precursors of the Hubbard bands [56]. When μ reaches the edge of the lower Bogoliubov peak, metallic behavior is recovered since doped holes appear at $\omega = 0$. The rearrangement of the spectral weight is not expected from the HF Slater solution. Upon doping, spectral weight transfers from high to low frequencies: The lower Bogoliubov peak decreases in intensity and moves close to the Fermi energy $\omega = 0$ and, correspondingly, the upper Bogoliubov peak broadens. Figure 3(b) shows that

the upper and lower Bogoliubov peaks have a sizable spin polarization, as in the $t' = 0$ case [37].

By contrast, for $U = 12$, the spectra for $\delta = 0$ in Figs. 3(c) and 3(d) have a clear four-peak structure: two Bogoliubov peaks surrounded by Hubbard bands [37,52,56,57]. In the doped case, there is a dramatic redistribution of spectral weight over a large frequency range across the AF gap, reminiscent of the Eskes-Meinders-Sawatzky picture [58]: The lower Bogoliubov peak sharpens and a new spectral feature, an "in-gap state," appears between the upper Hubbard band and the Fermi level located at $\omega = 0$. In that picture, the lower Hubbard band comes mostly from removing electrons in singly occupied sites, while the upper Hubbard band comes mostly from adding electrons to singly occupied sites. Given the large local moment at this value of U in the AF, this is consistent with the fact that these Hubbard bands are strongly spin
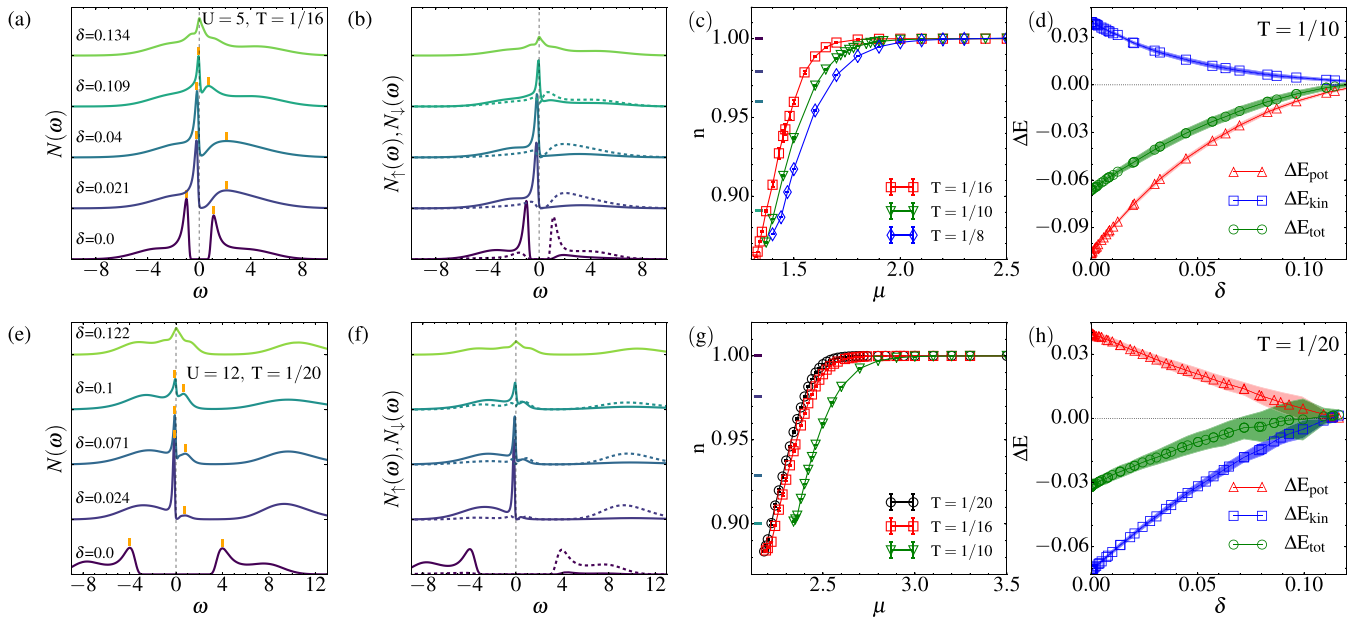

FIG. 3. Local DOS (a), (e) along with spin projections (b), (f) for different doping levels as obtained from analytically continued [55] data. Vertical bars indicate the position of the Bogoliubov peaks. Occupation vs chemical potential $n(\mu) = 1 - \delta(\mu)$ for different temperatures (c), (g). Horizontal ticks mark the values of dopings that correspond to the values shown in (a), (e). Doping dependence of the difference in potential, kinetic, and total energies between the AF and the underlying normal phase (d), (h). Data are for $t' = -0.1$ and $U = 5$ (top panels) and $U = 12$ (bottom panels). For more data on $N(\omega)$, see Figs. 4 and 5 in SM [35].

polarized, as seen in Fig. 3(f). On the other hand, the in-gap states come, in that same picture [58], from adding electrons in empty sites, which explains the near absence of spin polarization observed in Fig. 3(f). Finally, with further doping, the lower Bogoliubov peak and the Hubbard bands decrease in intensity at the expense of the in-gap state above $\omega = 0$. These results are compatible with the variational approach in Ref. [59].

Stability of the Néel phase. To assess the origin of the stability of the AF phase, we compare the kinetic, potential, and total energy differences between the AF phase and the underlying normal phase [22,37,60] as a function of doping δ at low T. Figures 3(d) and 3(h) show that the crossover in the source of stability of the AF phase that we identified earlier [37] at $\delta = 0$ persists for all doping levels. Therefore, the hidden Mott transition at $\delta = 0$ reorganizes the energetics both of the AF-I at $\delta = 0$ and of the AF-M away from $\delta = 0$.

Discussion. Our results are relevant for experiments with ultracold atoms in a spatially homogenous region and with cuprates. The first observation of the AF phase in a 2D square optical lattice appeared recently [14]. Persistence of AF correlations was found up to $\delta \approx 0.15$ for $U = 7.2$ and $t' = 0$. The consistency of this finding with our results is promising. Our U-δ-T map of the AF phase can be explored further with ultracold-atom systems since U, δ, and T can be tuned. Specifically, the nonmonotonic behavior of $\delta_N^d(U)$, along with a stronger reduction of $T_N^d(U)$ with increasing $|t'|$ at small U, are testable predictions.

When comparing our U-T-δ map with experiments on hole-doped cuprates, one should focus on the multilayer case where interlayer magnetic exchange favors mean-field-like behavior. In the $n = 5$ CuO_2 layer cuprates, AF persists up to $\delta \approx 0.10$ and it decreases with decreasing n [61,62]. Our predictions for m_z could be compared with neutron scattering and muon spin rotation experiments in this regime. Other effects that we did not take into account and that can decrease $\delta_N^d(U)$ are

the development of incommensurate spin-density waves and competition with other phases.

The $n(\mu)$ curve and the resulting charge compressibility κ that describes the continuous transition between an AF insulator and an AF metal as a function of doping is another prediction that can be tested with ultracold atoms. In principle, such measurements are also possible in cuprates [63–66].

The in-gap state feature that we found in the DOS has a position and a width that is compatible with recent scanning tunneling microscopy experiments on lightly doped AF Mott insulators [16,17]. In addition, the observed transfer of spectral weight from high energy to low energy as a function of doping is consistent with our results. We predict that a spin-polarized scanning tunneling microscopy (STM) probe will find that these states are essentially unpolarized, by contrast with the lower and upper Hubbard bands [67].

Our prediction that the doped AF state is stabilized by a gain in kinetic energy for large U and by a gain in potential energy for small U can in principle be tested by optical spectroscopy in cuprates [68–70]. If the correlation strength U is lower in electron-doped than in hole-doped cuprates, as has been proposed [71,72], our data suggest a potential energy-driven AF in electron-doped cuprates and a kinetic energy-driven AF in hole-doped cuprates, similar to earlier findings on the Emery model [73].

Moving forwards, it will be important to study the interplay between antiferromagnetism, pseudogap, and superconductivity [74–79].

[1] B. Keimer, S. A. Kivelson, M. R. Norman, S. Uchida, and J. Zaanen, Nature (London) **518**, 179 (2015).

[2] P. W. Anderson, Science **235**, 1196 (1987).

[3] D. Jaksch and P. Zoller, Ann. Phys. **315**, 52 (2005).

[4] A.-M. S. Tremblay, in *Emergent Phenomena in Correlated Matter Modeling and Simulation*, edited by E. Pavarini, E. Koch, and U. Schollwöck (Verlag des Forschungszentrum, Jülich, 2013), Vol. 3, Chap. 10.

[5] A. Georges and T. Giamarchi, in *Many-Body Physics with Ultracold Gases*, edited by C. Salomon, G. Shlyapnikov, and L. Cugliandolo, Lecture Notes of the Les Houches Summer School Vol. 94, July 2010 (Oxford University Press, Oxford, UK, 2010), Chap. 1.

[6] T. Maier, M. Jarrell, T. Pruschke, and M. H. Hettler, Rev. Mod. Phys. **77**, 1027 (2005).

[7] G. Kotliar, S. Y. Savrasov, K. Haule, V. S. Oudovenko, O. Parcollet, and C. A. Marianetti, Rev. Mod. Phys. **78**, 865 (2006).

[8] A.-M. S. Tremblay, B. Kyung, and D. Sénéchal, Low Temp. Phys. **32**, 424 (2006).

[9] D. Greif, T. Uehlinger, G. Jotzu, L. Tarruell, and T. Esslinger, Science **340**, 1307 (2013).

[10] R. A. Hart, P. M. Duarte, T.-L. Yang, X. Liu, T. Paiva, E. Khatami, R. T. Scalettar, N. Trivedi, D. A. Huse, and R. G. Hulet, Nature (London) **519**, 211 (2015).

[11] M. F. Parsons, A. Mazurenko, C. S. Chiu, G. Ji, D. Greif, and M. Greiner, Science **353**, 1253 (2016).

[12] M. Boll, T. A. Hilker, G. Salomon, A. Omran, J. Nespolo, L. Pollet, I. Bloch, and C. Gross, Science **353**, 1257 (2016).

[13] L. W. Cheuk, M. A. Nichols, K. R. Lawrence, M. Okan, H. Zhang, E. Khatami, N. Trivedi, T. Paiva, M. Rigol, and M. W. Zwierlein, Science **353**, 1260 (2016).

[14] A. Mazurenko, C. S. Chiu, G. Ji, M. F. Parsons, M. Kanász-Nagy, R. Schmidt, F. Grusdt, E. Demler, D. Greif, and M. Greiner, Nature (London) **545**, 462 (2017).

[15] J. H. Drewes, L. A. Miller, E. Cocchi, C. F. Chan, N. Wurz, M. Gall, D. Pertot, F. Brennecke, and M. Köhl, Phys. Rev. Lett. **118**, 170401 (2017).

[16] P. Cai, W. Ruan, Y. Peng, C. Ye, X. Li, Z. Hao, X. Zhou, D.-H. Lee, and Y. Wang, Nat. Phys. **12**, 1047 (2016).

[17] C. Ye, P. Cai, R. Yu, X. Zhou, W. Ruan, Q. Liu, C. Jin, and Y. Wang, Nat. Commun. **4**, 1365 (2013).

[18] K. Borejsza and N. Dupuis, Phys. Rev. B **69**, 085119 (2004).

[19] D. Sénéchal, P.-L. Lavertu, M.-A. Marois, and A.-M. S. Tremblay, Phys. Rev. Lett. **94**, 156404 (2005).

[20] M. Aichhorn and E. Arrigoni, Europhys. Lett. **72**, 117 (2005).

[21] M. Aichhorn, E. Arrigoni, M. Potthoff, and W. Hanke, Phys. Rev. B **76**, 224509 (2007).

[22] L. F. Tocchio, F. Becca, and S. Sorella, Phys. Rev. B **94**, 195126 (2016).

[23] B.-X. Zheng and G. K.-L. Chan, Phys. Rev. B **93**, 035126 (2016).

[24] J. E. Hirsch, Phys. Rev. B **31**, 4403 (1985).

[25] S. R. White, D. J. Scalapino, R. L. Sugar, E. Y. Loh, J. E. Gubernatis, and R. T. Scalettar, Phys. Rev. B **40**, 506 (1989).

[26] A. I. Lichtenstein and M. I. Katsnelson, Phys. Rev. B **62**, R9283 (2000).

[27] T. Paiva, R. T. Scalettar, C. Huscroft, and A. K. McMahan, Phys. Rev. B **63**, 125116 (2001).

[28] B. Kyung, S. S. Kancharla, D. Sénéchal, A.-M. S. Tremblay, M. Civelli, and G. Kotliar, Phys. Rev. B **73**, 165114 (2006).

[29] T. Paiva, R. Scalettar, M. Randeria, and N. Trivedi, Phys. Rev. Lett. **104**, 066406 (2010).

[30] T. Sato and H. Tsunetsugu, Phys. Rev. B **94**, 085110 (2016).

[31] T. Ayral and O. Parcollet, Phys. Rev. B **92**, 115109 (2015).

[32] T. Ayral and O. Parcollet, Phys. Rev. B **93**, 235124 (2016).

[33] T. Ayral and O. Parcollet, Phys. Rev. B **94**, 075159 (2016).

[34] G. Rohringer, H. Hafermann, A. Toschi, A. A. Katanin, A. E. Antipov, M. I. Katsnelson, A. I. Lichtenstein, A. N. Rubtsov, and K. Held, arXiv:1705.00024.

[35] See Supplemental Material at http://link.aps.org/supplemental/10.1103/PhysRevB.96.241109 for the staggered magnetization curves as a function of U and δ for few temperatures, average sign, and complementary data for the local DOS.

[36] A. Georges, G. Kotliar, W. Krauth, and M. J. Rozenberg, Rev. Mod. Phys. **68**, 13 (1996).

[37] L. Fratino, P. Sémon, M. Charlebois, G. Sordi, and A.-M. S. Tremblay, Phys. Rev. B **95**, 235109 (2017).

[38] E. Gull, A. J. Millis, A. I. Lichtenstein, A. N. Rubtsov, M. Troyer, and P. Werner, Rev. Mod. Phys. **83**, 349 (2011).

[39] P. Sémon, C.-H. Yee, K. Haule, and A.-M. S. Tremblay, Phys. Rev. B **90**, 075149 (2014).

[40] P. Sémon and A.-M. S. Tremblay, Phys. Rev. B **85**, 201101 (2012).

[41] P. Sémon, G. Sordi, and A.-M. S. Tremblay, Phys. Rev. B **89**, 165113 (2014).

[42] N. D. Mermin and H. Wagner, Phys. Rev. Lett. **17**, 1133 (1966).

[43] P. C. Hohenberg, Phys. Rev. **158**, 383 (1967).

[44] J. R. Schrieffer, X. G. Wen, and S. C. Zhang, Phys. Rev. B **39**, 11663 (1989).

[45] A. Georges and W. Krauth, Phys. Rev. B **48**, 7167 (1993).

[46] J. K. Freericks and M. Jarrell, Phys. Rev. Lett. **74**, 186 (1995).

[47] W. Hofstetter and D. Vollhardt, Ann. Phys. **7**, 48 (1998).

[48] R. Chitra and G. Kotliar, Phys. Rev. Lett. **83**, 2386 (1999).

[49] R. Zitzler, N.-H. Tong, T. Pruschke, and R. Bulla, Phys. Rev. Lett. **93**, 016406 (2004).

[50] J. Kanamori, Prog. Theor. Phys. **30**, 275 (1963).

[51] K. A. Brueckner, T. Soda, P. W. Anderson, and P. Morel, Phys. Rev. **118**, 1442 (1960).

[52] Y. M. Vilk and A.-M. S. Tremblay, J. Phys. I (France) **7**, 1309 (1997).

[53] I. Yang, E. Lange, and G. Kotliar, Phys. Rev. B **61**, 2521 (2000).

[54] A. Camjayi, R. Chitra, and M. J. Rozenberg, Phys. Rev. B **73**, 041103 (2006).

[55] D. Bergeron and A.-M. S. Tremblay, Phys. Rev. E **94**, 023303 (2016).

[56] A. Moreo, S. Haas, A. W. Sandvik, and E. Dagotto, Phys. Rev. B **51**, 12045 (1995).

[57] R. Preuss, W. Hanke, and W. von der Linden, Phys. Rev. Lett. **75**, 1344 (1995).

[58] H. Eskes, M. B. J. Meinders, and G. A. Sawatzky, Phys. Rev. Lett. **67**, 1035 (1991).

[59] H.-K. Wu and T.-K. Lee, Phys. Rev. B **95**, 035133 (2017).

[60] C. Taranto, G. Sangiovanni, K. Held, M. Capone, A. Georges, and A. Toschi, Phys. Rev. B **85**, 085124 (2012).

[61] H. Mukuda, Y. Yamaguchi, S. Shimizu, Y. Kitaoka, P. Shirage, and A. Iyo, J. Phys. Soc. Jpn. **77**, 124706 (2008).

[62] H. Mukuda, S. Shimizu, A. Iyo, and Y. Kitaoka, J. Phys. Soc. Jpn. **81**, 011008 (2012).

[63] A. Ino, T. Mizokawa, A. Fujimori, K. Tamasaku, H. Eisaki, S. Uchida, T. Kimura, T. Sasagawa, and K. Kishio, Phys. Rev. Lett. **79**, 2101 (1997).

[64] N. Harima, A. Fujimori, T. Sugaya, and I. Terasaki, Phys. Rev. B **67**, 172501 (2003).

[65] G. Rietveld, N. Y. Chen, and D. van der Marel, Phys. Rev. Lett. **69**, 2578 (1992).

[66] D. van der Marel and G. Rietveld, Phys. Rev. Lett. **69**, 2575 (1992).

[67] In these experiments, the DOS at $\omega = 0$ vanishes while in our case it is small. The inhomogeneity of the samples suggests that disorder can induce localization effects at $\omega = 0$, as pointed out in Ref. [59]. The AF phase of cuprates at finite doping is generally considered metallic [80].

[68] H. J. A. Molegraaf, C. Presura, D. van der Marel, P. H. Kes, and M. Li, Science **295**, 2239 (2002).

[69] G. Deutscher, A. F. Santander-Syro, and N. Bontemps, Phys. Rev. B **72**, 092504 (2005).

[70] F. Carbone, A. B. Kuzmenko, H. J. A. Molegraaf, E. van Heumen, V. Lukovac, F. Marsiglio, D. van der Marel, K. Haule, G. Kotliar, H. Berger, S. Courjault, P. H. Kes, and M. Li, Phys. Rev. B **74**, 064510 (2006).

[71] D. Sénéchal and A.-M. S. Tremblay, Phys. Rev. Lett. **92**, 126401 (2004).

[72] C. Weber, K. Haule, and G. Kotliar, Nat. Phys. **6**, 574 (2010).

[73] C. Weber, K. Haule, and G. Kotliar, Phys. Rev. B **82**, 125107 (2010).

[74] G. Sordi, K. Haule, and A.-M. S. Tremblay, Phys. Rev. Lett. **104**, 226402 (2010).

[75] G. Sordi, K. Haule, and A.-M. S. Tremblay, Phys. Rev. B **84**, 075161 (2011).

[76] G. Sordi, P. Sémon, K. Haule, and A.-M. S. Tremblay, Sci. Rep. **2**, 547 (2012).

[77] G. Sordi, P. Sémon, K. Haule, and A.-M. S. Tremblay, Phys. Rev. B **87**, 041101 (2013).

[78] L. Fratino, P. Sémon, G. Sordi, and A.-M. S. Tremblay, Sci. Rep. **6**, 22715 (2016).

[79] L. Fratino, P. Sémon, G. Sordi, and A.-M. S. Tremblay, Phys. Rev. B **93**, 245147 (2016).

[80] Y. Ando, A. N. Lavrov, S. Komiya, K. Segawa, and X. F. Sun, Phys. Rev. Lett. **87**, 017001 (2001).